Structures and Stabilities of Ternary Copper(II) Complexes Containing an Acidic and a Basic Amino Acid. Evidence for Arginine Side Chain Involvement in Intermolecular Interactions and Its Biological Implication

Hideki Masuda,† Akira Odani, Takayasu Yamazaki, Tatsuo Yajima, and Osamu Yamauchi*

Department of Chemistry, Faculty of Science, Nagoya University, Chikusa-ku, Nagoya 464-01, Japan

Received April 27, 1992

Ternary copper(II) complexes containing an acidic amino acid (A) and a basic amino acid (B), Cu(A)(B), where A refers to ethylenediamine-*N*-monoacetic acid (EDMA) and DL-2,3-diaminopropionic acid (DAP) and B to L-arginine (L-Arg) and L-lysine (L-Lys), have been investigated by absorption and circular dichroism (CD) spectral, solution equilibrium, and X-ray diffraction methods with emphasis on ligand–ligand interactions. Deviations of the CD spectral magnitudes from additivity were observed for the systems Cu(A)(B) where ligand–ligand hydrogen bonds or electrostatic interactions exist between the oppositely charged side chains. Evaluation of the stability enhancement by such intramolecular interactions has been made by considering the following hypothetical equilibrium (charges are omitted): Cu(A)(B′) + Cu(A′)(B) ⇌ Cu(A)(B) + Cu(A′)(B′) (*K*), where A′ and B′ are ligands without an interacting side chain group such as valine (Val) and ethylenediamine, respectively, and ligand–ligand interactions are possible only in Cu(A)(B). The log *K* value which is defined to be equal to zero in the absence of interactions was calculated for each Cu(A)(B) from the overall stability constants of the relevant ternary complexes determined at 25 °C and I = 0.1 M (KNO_3) to be in the order Cu(DAP)(L-Arg) (0.63) > Cu(EDMA)(L-Arg) (0.15) ~ Cu(EDMA)(L-Lys) (0.14) ~ Cu(DAP)(L-Lys) (0.16) > Cu(EDMA)(L-Val) ~ Cu(DAP)(L-Val) ~ 0. The stability difference between Cu(EDMA)(L-Arg) and Cu(DAP)(L-Arg) was inferred to be due to steric requirements for intramolecular ligand–ligand interactions. X-ray crystal structure analysis has been performed on [Cu(EDMA)(L-Arg)ClO_4]·$^1/_2C_2H_5OH$ (**1**) and [Cu(L-Arg)$_2$]$(NO_3)_2$·$3H_2O$ (**2**). Complex **1** crystallizes in the orthorhombic space group $P2_12_12_1$ with four molecules in a unit cell of dimensions a = 7.824(3) Å, b = 24.979(3) Å, and c = 10.617(4) Å. The Cu(II) ion is in a slightly distorted square-pyramidal geometry with the two nitrogen atoms of EDMA and the nitrogen and oxygen atoms of L-Arg coordinated at the equatorial positions and the carboxylate oxygen atom of EDMA coordinated at an axial position. A perchlorate oxygen atom weakly coordinates at the other axial site. The coordinated carboxylate group of EDMA is hydrogen-bonded to the positively charged guanidinium group of L-Arg of a neighboring complex molecule with the N···O distances of 2.89 and 2.85 Å. Complex **2** crystallizes in the monoclinic space group $C2$ with four molecules in a unit cell of dimensions a = 26.680(3) Å, b = 7.320(1) Å, c = 12.772(1) Å, and β = 92.08(1)°. The Cu(II) ion has a square-planar geometry with the two nitrogen and two oxygen atoms of two coordinated L-Arg molecules in a cis configuration with respect to the amino groups, which are hydrogen-bonded to an uncoordinated nitrate ion. The side chain guanidinium group is also hydrogen-bonded to two uncoordinated nitrate ions with the N···O distances of 2.84–2.97 Å. On the basis of the log *K* values and the crystal structures, intermolecular interactions involving the arginine guanidinium group were inferred to be more specific than those involving the lysine ammonium group, and their biological implication was discussed.

Introduction

Biological reactions are characterized by high efficiency and specificity, which are achieved by molecular recognition, structural fitness, and organized molecular arrangement such as in membranes.[1] Specific bondings in biological systems such as enzyme–substrate complexes result from molecular recognition by a combination of weak interactions at or near the active site.[2] A classical example is the complex of the zinc enzyme carboxypeptidase A (CPA) with the model substrate glycyl-L-tyrosine, in which the guanidinium group of arginine 145 of CPA and a hydrophobic pocket interact with the carboxylate and the tyrosine phenol group of the substrate, respectively, to fix it in a specific way around the central zinc ion.[3] Electrostatic interactions are responsible for the substrate specificity of trypsin.[4]

Much attention has been paid recently to the sequence-specific DNA-binding proteins.[5-7] The recent X-ray crystal structure analysis of a complex of a peptide that contains the DNA-binding domain from Zif268 and a consensus DNA-binding site[8] has revealed the existence of zinc finger–DNA binding through weak interactions, especially between the guanine base of DNA and the Arg guanidinium and histidine imidazole groups of the zinc-

† Present address: Department of Applied Chemistry, Nagoya Institute of Technology, Showa-ku, Nagoya 466, Japan.

(1) Alberts, B.; Bray, D.; Lewis, J.; Raff, M.; Roberts, K.; Watson, J. D. *Molecular Biology of the Cell*, 2nd ed.; Garland Publishing: New York, 1989; pp 122–132.
(2) (a) Frieden, E. *J. Chem. Educ.* **1975**, *52*, 754–761. (b) Jencks, W. P. *Adv. Enzymol. Relat. Areas Mol. Biol.* **1975**, *43*, 219–410.
(3) (a) Quiocho, F. A.; Lipscomb, W. N. *Adv. Protein Chem.* **1971**, *25*, 1–78. (b) Christianson, D. W.; Lipscomb, W. N. *Acc. Chem. Res.* **1989**, *22*, 62–69.
(4) Huber, R.; Bode, W. *Acc. Chem. Res.* **1978**, *11*, 114–122.
(5) Miller, J.; McLachlan, A. D.; Klug, A. *EMBO J.* **1985**, *4*, 1609–1614.
(6) Brown, R. S.; Sander, C.; Argos, P. *FEBS Lett.* **1985**, *186*, 271–274.
(7) Berg, J. M. *Met. Ions Biol. Syst.* **1989**, *25*, 235–254.
(8) Pavletich, N. P.; Pabo, C. O. *Science* **1991**, *252*, 809–817.
(9) (a) Yamauchi, O.; Nakao, Y.; Nakahara, A. *Bull. Chem. Soc. Jpn.* **1975**, *48*, 2572–2578. (b) Sakurai, T.; Yamauchi, O.; Nakahara, A. *Bull. Chem. Soc. Jpn.* **1976**, *49*, 169–173. (c) Sakurai, T.; Yamauchi, O.; Nakahara, A. *Bull. Chem. Soc. Jpn.* **1976**, *49*, 1579–1584. (d) Yamauchi, O.; Odani, A. *J. Am. Chem. Soc.* **1981**, *103*, 391–398. (e) Odani, A.; Yamauchi, O. *Bull. Chem. Soc. Jpn.* **1981**, *54*, 3773–3779. (f) Yamauchi, O. *J. Mol. Catal.* **1984**, *23*, 255–261. (g) Yamauchi, O.; Odani, A. *Inorg. Chim. Acta* **1985**, *100*, 165–172. (h) Yamauchi, O.; Odani, A. *J. Am. Chem. Soc.* **1985**, *107*, 5938–5945. (i) Odani, A.; Deguchi, S.; Yamauchi, O. *Inorg. Chem.* **1986**, *25*, 62–69. (j) Odani, A.; Yamauchi, O. *Nippon Kagaku Kaishi* **1987**, 336–344. (k) Yamauchi, O.; Odani, A. *Nippon Kagaku Kaishi* **1988**, 369–382. (l) Masuda, H.; Matsumoto, O.; Odani, A.; Yamauchi, O. *Nippon Kagaku Kaishi* **1988**, 783–788. (m) Yamauchi, O.; Odani, A.; Kohzuma, T.; Masuda, H.; Toriumi, K.; Saito, K. *Inorg. Chem.* **1989**, *28*, 4066–4068. (n) Yamauchi, O.; Odani, A.; Masuda, H. *Inorg. Chim. Acta* **1992**, *198–200*, 749–761.

0020-1669/93/1332-1111$04.00/0 © 1993 American Chemical Society

Scheme I. Intra- and Intermolecular Interactions in Cu(A)(B)

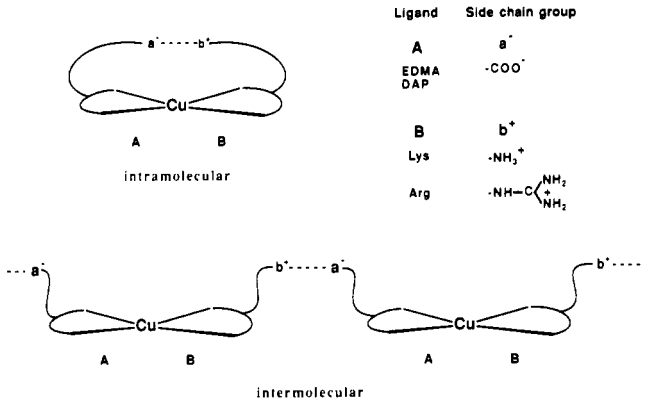

finger domain. These findings present possibilities of a variety of specific intermolecular interactions between proteins and nucleic acids, as well as between enzymes and substrates. Because of the weakness of such interactions, however, information on their mode and energy is lacking.

We have been studying weak interactions in ternary Cu(II) and Pd(II) complexes[9] and in Pt(II) complex–nucleotide systems[10] as models for metalloenzyme–substrate and intercalator–DNA interactions, respectively, by spectroscopic, thermodynamic, and X-ray diffraction methods. The existence in solution of electrostatic interactions in ternary Cu(II) and Pd(II) complexes involving an acidic and a basic amino acid has been concluded from their circular dichroism (CD) and ^{1}H NMR spectra and isolation of various ternary complexes.[9a-d,k,n] Stability increases in several ternary amino acid–Cu(II) complexes have been ascribed to electrostatic ligand–ligand interactions.[11] Intramolecular aromatic ring stacking in Cu(II)– and Pd(II)–heteroaromatic ligand–aromatic amino acid (or dipeptide) complexes concluded from spectral and solution equilibrium studies has been established in the solid state by X-ray crystal structure analysis of Cu(phen)(L-Trp),[9l,12] Cu(histamine)(L-Phe and L-Tyr),[9m] Cu(bpy)(L-Tyr),[9n] and Cu(bpy)(L-Trp)[13] (phen = 1,10-phenanthroline; bpy = 2,2′-bipyridine; Trp = tryptophan; Phe = phenylalanine; Tyr = tyrosine). With a view to elucidating the importance of the Arg and Lys residues in the mechanisms of specific interactions in biological systems, we studied the properties of the ternary Cu(II) complexes Cu(A)(B) shown in Scheme I with expectation of finding electrostatic ligand–ligand interactions between the oppositely charged side chain groups of the ligands. For this purpose, we selected such pairs of A and B as would exhibit the mentioned interactions as well as the pairs without any interactions and investigated the structures and spectral and thermodynamic properties of Cu(A)(B). For convenience, ethylenediamine (en), ethylenediamine-*N*-monoacetic acid (EDMA), and DL-2,3-diaminopropionic acid (DAP) will be referred to as A ligands and L-Arg, L-Lys, L-alanine (L-Ala), and L-valine (L-Val) as B ligands, where Arg is treated as having a positive charge in the side chain in the pH range studied.

The present investigations have revealed the complex stability enhancement due to such interactions and the mode of the guanidinium–carboxylate bonding between the side chains of the Cu(EDMA)(L-Arg) molecules in the solid state, which is to our knowledge the first example of intermolecular interactions between ligand side chains involving a guanidinium group. The crystal structure of $[Cu(L\text{-}Arg)_2](NO_3)_2\cdot 3H_2O$ showing guanidinium–nitrate bonds is presented as a further example. We here report the structures and stabilities of the ternary complexes Cu(A)(B), as well as a discussion of the stability enhancement due to the interactions and the biological relevance with emphasis on the Arg guanidinium group.

Table I. Crystal Data for $[Cu(EDMA)(L\text{-}Arg)(ClO_4)]\cdot{}^1/_2C_2H_5OH$ (**1**) and $[Cu(L\text{-}Arg)_2](NO_3)_2\cdot 3H_2O$ (**2**)

	1	**2**
formula	$CuC_{11}H_{26}N_6O_{8.5}Cl$	$CuC_{12}H_{22}N_{10}O_{13}$
fw	477.36	577.91
cryst syst	orthorhombic	monoclinic
space group	$P2_12_12_1$	$C2$
a/Å	7.824(3)	26.680(3)
b/Å	24.979(3)	7.320(1)
c/Å	10.617(4)	12.772(1)
β/deg		92.08(1)
V/Å^3	2074.8	2497.5
Z	4	4
ρ/g cm^{-3}	1.529	1.537
μ/cm^{-1}	34.41	19.11
$F(000)$	1256	1188
cryst size/mm	0.05 × 0.01 × 0.01	0.1 × 0.2 × 0.2
λ(Cu Kα)/Å	1.541 78	1.541 78
2θ limit/deg	110	120
No. of reflns used ($\|F_o\| > 3\sigma(\|F_o\|)$)	1152	1380
range of h,k,l	±9,+25,+11	+38,+10,±18
R^a	0.0987	0.0398
$R_w{}^b$	0.0831	0.0459

^{a} $R = \sum(\|F_o\| - |F_c\|)/\sum|F_o|$. ^{b} $R_w = [\sum w(|F_o| - |F_c|)^2/\sum w(F_o)^2]^{1/2}$, $w^{-1} = [\sigma^2(F_o) + (0.015F_o)^2]$.

Experimental Section

Materials. L-Arg, L-Lys·HCl, L-Ala, and L-Val were purchased from Nacalai Tesque. EDMA was obtained from Tokyo Kasei, and DL-DAP, from Sigma. All the chemicals used were of reagent grade or of highest grade available. Water was distilled, deionized, and further purified by a Milli-Q Labo.

Synthesis of $[Cu(L\text{-}Arg)_2](NO_3)_2\cdot 3H_2O$ (2). To an aqueous solution of Arg·HCl (0.84 g, 4.0 mmol) was added an aqueous solution of $Cu(NO_3)_2\cdot 3H_2O$ (0.48 g, 2.0 mmol), and the pH of the resulting solution was adjusted to 6.5 with 1 M NaOH. Blue crystals of **2** which separated upon standing at room temperature were collected and dried. Yield: 0.33 g (28%).

Determination of Stability Constants. pH titrations were carried out at 25 °C and I = 0.1 M (KNO_3) under a nitrogen atmosphere in the same way as described previously[9h,14] for solutions of binary and ternary systems containing Cu(II), A, and B in the molar ratios of 1:1~2:0, 1:0:2, 1:1:1, with an appropriate amount of HNO_3. The concentrations of the samples were 1–2 mM with respect to Cu(II). pH values were measured with an Orion EA-920 or a Beckman pHI-71 pH meter, both equipped with a Beckman 39314 glass electrode and a 39419 double-junction reference electrode. Calibration of the pH meter was made with NBS standard buffer solutions (pH 4.008, 7.413, and 9.180 at 25 °C). Several titrations were carried out for each system, for which about 200–300 data points were collected. The stability constants β_{pqrs} defined by eq 1 (charges are

$$pCu + qA + rB + sH \overset{\beta_{pqrs}}{\rightleftharpoons} Cu_p(A)_q(B)_rH_s$$

$$\beta_{pqrs} = \frac{[Cu_p(A)_q(B)_rH_s]}{[Cu]^p[A]^q[B]^r[H]^s} \qquad (1)$$

omitted for simplicity) were calculated by using the program SUPER-

(10) (a) Yamauchi, O.; Odani, A.; Shimata, R.; Y. Kosaka. *Inorg. Chem.* **1986**, *25*, 3337–3339. (b) Yamauchi, O.; Odani, A.; Shimata, R.; Ishiguro, S. *Recl. Trav. Chim. Pays-Bas* **1987**, *106*, 196–197. (c) Masuda, H.; Yamauchi, O. *Inorg. Chim. Acta* **1987**, *136*, L29–L31. (d) Odani, A.; Shimata, R.; Masuda, H.; Yamauchi, O. *Inorg. Chem.* **1991**, *30*, 2133–2138. (e) Odani, A.; Masuda, H. Yamauchi, O.; Ishiguro, S. *Inorg. Chem.* **1991**, *30*, 4484–4486.
(11) (a) Brookes, G.; Pettit, L. D. *J. Chem. Soc., Dalton Trans.* **1977**, 1918–1924. (b) Sigel, H. In *Coordination Chemistry-20*; Benerjea, D., Ed.; Pergamon: Oxford, U.K., 1980; pp 27–45. (c) Tribolet, R.; Sigel, H.; Trefzer, K. *Inorg. Chim. Acta* **1983**, *79*, 278–280.
(12) Aoki, K.; Yamazaki, H. *J. Chem. Soc., Dalton Trans.* **1987**, 2017–2021.
(13) Masuda, H.; Sugimori, T.; Odani, A.; Yamauchi, O. *Inorg. Chim. Acta* **1991**, *180*, 73–79.
(14) Yamauchi, O.; Seki, H.; Shoda, T. *Bull. Chem. Soc. Jpn.* **1983**, *56*, 3258–3267.

Table II. Bond Lengths (Å) and Angles (deg) for [Cu(EDMA)(L-Arg)](ClO_4)·C_2H_5OH (**1**)

Cu–O(1)	1.932(13)	Cu–O(3)	2.337(13)
Cu–N(1)	2.018(17)	Cu–N(2)	1.988(16)
Cu–N(3)	1.995(15)	Cl–O(5)	1.424(17)
Cl–O(6)	1.418(18)	Cl–O(7)	1.404(17)
Cl–O(8)	1.395(18)	O(1)–C(1)	1.280(22)
O(2)–C(1)	1.231(22)	O(3)–C(10)	1.266(22)
O(4)–C(10)	1.288(23)	N(1)–C(2)	1.475(25)
N(2)–C(7)	1.503(28)	N(3)–C(8)	1.501(24)
N(3)–C(9)	1.477(26)	N(4)–C(5)	1.438(28)
N(4)–C(6)	1.341(26)	N(5)–C(6)	1.328(23)
N(6)–C(6)	1.302(26)	C(1)–C(2)	1.533(30)
C(2)–C(3)	1.553(29)	C(3)–C(4)	1.480(27)
C(4)–C(5)	1.532(29)	C(7)–C(8)	1.416(34)
C(9)–C(10)	1.55(9)	O(1E)–C(2E)	1.16(8)
C(1E)–C(2E)	1.51(9)		
O(1)–Cu–O(3)	89.9(5)	O(1)–Cu–N(1)	83.4(6)
O(1)–Cu–N(2)	164.8(6)	O(1)–Cu–N(3)	92.0(6)
O(3)–Cu–N(1)	100.1(6)	O(3)–Cu–N(2)	103.6(6)
O(3)–Cu–N(3)	76.5(5)	N(1)–Cu–N(2)	100.7(7)
N(1)–Cu–N(3)	174.3(7)	N(2)–Cu–N(3)	84.6(6)
O(5)–Cl–O(6)	107.4(10)	O(5)–Cl–O(7)	106.8(10)
O(5)–Cl–O(8)	112.1(10)	O(6)–Cl–O(7)	109.3(11)
O(6)–Cl–O(8)	110.1(11)	O(7)–Cl–O(8)	111.0(11)
Cu–O(1)–C(1)	116.4(12)	Cu–O(3)–C(10)	108.3(12)
Cu–N(1)–C(2)	111.2(12)	Cu–N(2)–C(7)	108.7(13)
Cu–N(3)–C(8)	106.2(11)	Cu–N(3)–C(9)	110.9(12)
C(8)–N(3)–C(9)	111.5(14)	C(5)–N(4)–C(6)	127.1(17)
O(1)–C(1)–O(2)	120.0(20)	O(1)–C(1)–C(2)	118.5(16)
O(2)–C(1)–C(2)	120.5(16)	N(1)–C(2)–C(1)	108.3(16)
N(1)–C(2)–C(3)	110.6(17)	C(1)–C(2)–C(3)	111.0(16)
C(2)–C(3)–C(4)	109.0(15)	C(3)–C(4)–C(5)	113.0(17)
N(4)–C(5)–C(4)	110.0(17)	N(4)–C(6)–N(5)	118.6(17)
N(4)–C(6)–N(6)	121.1(17)	N(5)–C(6)–N(6)	120.3(18)
N(2)–C(7)–C(8)	107.7(17)	N(3)–C(8)–C(7)	108.3(16)
N(3)–C(9)–C(10)	110.3(16)	O(3)–C(10)–O(4)	122.0(19)
O(3)–C(10)–C(9)	118.2(17)	O(4)–C(10)–C(9)	118.3(17)
O(1E)–C(2E)–C(1E)	134.1(51)		

Table III. Bond Lengths (Å) and Angles (deg) for [Cu(L-Arg)$_2$](NO_3)$_2$·$3H_2O$ (**2**)

Cu–O(1A)	1.930(4)	Cu–O(1B)	1.973(4)
Cu–N(2A)	1.974(5)	Cu–N(2B)	1.972(5)
O(1A)–C(1A)	1.302(9)	O(2A)–C(1A)	1.231(9)
O(1B)–C(1B)	1.282(8)	O(2B)–C(1B)	1.245(9)
N(2A)–C(2A)	1.498(9)	N(6A)–C(5A)	1.447(9)
N(6A)–C(7A)	1.338(12)	N(8A)–C(7A)	1.338(10)
N(9A)–C(7A)	1.333(13)	N(2B)–C(2B)	1.490(9)
N(6B)–C(5B)	1.478(10)	N(6B)–C(7B)	1.313(12)
N(8B)–C(7B)	1.299(12)	N(9B)–C(7B)	1.370(9)
C(1A)–C(2A)	1.528(10)	C(2A)–C(3A)	1.549(9)
C(3A)–C(4A)	1.481(11)	C(4A)–C(5A)	1.542(10)
C(1B)–C(2B)	1.520(10)	C(2B)–C(3B)	1.537(10)
C(3B)–C(4B)	1.505(11)	C(4B)–C(5B)	1.494(13)
N(11)–O(11)	1.241(11)	N(11)–O(12)	1.244(10)
N(11)–O(13)	1.259(8)	N(21)–O(21)	1.243(9)
N(21)–O(22)	1.260(10)	N(21)–O(23)	1.233(10)
O(1A)–Cu–O(1B)	94.3(2)	O(1A)–Cu–N(2A)	84.5(2)
O(1A)–Cu–N(2B)	175.2(4)	O(1B)–Cu–N(2A)	177.1(3)
O(1B)–Cu–N(2B)	84.3(2)	N(2A)–Cu–N(2B)	96.7(2)
Cu–O(1A)–C(1A)	114.4(4)	Cu–O(1B)–C(1B)	114.9(4)
Cu–N(2A)–C(2A)	108.2(4)	C(5A)–N(6A)–C(7A)	124.3(8)
Cu–N(2B)–C(2B)	110.6(4)	C(5B)–N(6B)–C(7B)	122.0(8)
O(1A)–C(1A)–O(2A)	122.0(7)	O(1A)–C(1A)–C(2A)	117.1(6)
O(2A)–C(1A)–C(2A)	120.9(7)	N(2A)–C(2A)–C(1A)	108.2(6)
N(2A)–C(2A)–C(3A)	112.0(6)	C(1A)–C(2A)–C(3A)	113.1(6)
C(2A)–C(3A)–C(4A)	112.2(6)	C(3A)–C(4A)–C(5A)	112.1(6)
N(6A)–C(5A)–C(4A)	115.2(6)	N(6A)–C(7A)–N(8A)	117.5(8)
N(6A)–C(7A)–N(9A)	123.0(7)	N(8A)–C(7A)–N(9A)	119.5(8)
O(1B)–C(1B)–O(2B)	122.0(7)	O(1B)–C(1B)–C(2B)	117.8(6)
O(2B)–C(1B)–C(2B)	120.1(6)	N(2B)–C(2B)–C(1B)	109.2(6)
N(2B)–C(2B)–C(3B)	111.0(7)	C(1B)–C(2B)–C(3B)	111.9(6)
C(2B)–C(3B)–C(4B)	113.4(6)	C(3B)–C(4B)–C(5B)	113.2(7)
N(6B)–C(5B)–C(4B)	112.0(7)	N(6B)–C(7B)–N(8B)	123.9(7)
N(6B)–C(7B)–N(9B)	117.2(8)	N(8B)–C(7B)–N(9B)	118.9(8)
O(11)–N(11)–O(12)	121.5(7)	O(11)–N(11)–O(13)	118.6(8)
O(12)–N(11)–O(13)	119.8(8)	O(21)–N(21)–O(22)	120.3(7)
O(21)–N(21)–O(23)	120.3(7)	O(22)–N(21)–O(23)	119.4(7)

QUAD[15] with the aid of a FACOM M-780 computer at the Nagoya University Computation Center. In eq 1 *p*, *q*, *r*, and *s* are the numbers of moles of Cu, A, B, and H, respectively, in the complex and negative *s* values refer to hydroxide ions. pH meter readings (pH_M) were converted to hydrogen ion concentrations [H^+] by the relation [H^+] = $10^{-pH_M}/0.855$, and the apparent ion product of water was 13.96.[16]

Spectral Measurements. Absorption spectra were taken on a Hitachi 330 spectrophotometer at room temperature, and CD spectra were obtained with a JASCO J-40CS spectropolarimeter in a 1 cm path length quartz cell. Samples for the measurements were freshly prepared at pH 8 in the desired Cu(II):ligand ratios, the concentrations of Cu(II) being 2–100 mM. Ionic strength (*I*) was not adjusted (*I* = var).

X-ray Structure Determination of [Cu(EDMA)(L-Arg)ClO_4]·$^1/_2C_2H_5OH$ (1) and [Cu(L-Arg)$_2$](NO_3)$_2$·$3H_2O$ (2). Complex **1** was synthesized in the manner reported previously.[9a] The deep blue needlelike crystals suitable for X-ray analysis were obtained by recrystallization from aqueous ethanol. The complex crystallizes in the orthorhombic crystal system, and the space group $P2_12_12_1$ was chosen on the basis of the systematic absences observed during the data collection and the asymmetry of L-Arg. Diffraction data were collected at 295 K with a Rigaku AFC-5R four-circle diffractometer having a rotating anode and using graphite-monochromated Cu Kα radiation (λ = 1.541 78 Å). The crystal data and details of the parameters associated with data collection are given in Table I. The unit cell parameters were derived from least-squares refinement of 25 well-centered reflections. The intensities of three standard reflections measured every 100 reflections showed no significant variations. Intensity data were collected by the ω–2θ scan technique. Reflection data were corrected for Lorentz and polarization effects. Absorption correction was not applied because of the small size of the crystal (0.05 × 0.01 × 0.01 mm) and the small absorption coefficient.

X-ray data collection for complex **2** was performed in a manner similar to that above for deep blue platelike crystals suitable for X-ray analysis, which were obtained by recrystallization from water (Table I). The complex crystallizes in the monoclinic crystal system. The chiral space group *C*2 was chosen on the basis of the systematic absences observed during the data collection and asymmetry of L-Arg.

The structures were solved by the heavy-atom method and refined anisotropically for non-hydrogen atoms by full-matrix least-squares calculations. All hydrogen atoms were included as isotropic in the structure factor calculations at the final stage of refinement; their positions for **1** were located on the calculated positions except those for the ethanol molecule, and those for **2** were obtained from difference Fourier synthesis. The final *R* and R_w values were 0.0987 and 0.0831, respectively, for **1** and 0.0398 and 0.0459, respectively, for **2**. The weighting scheme $w^{-1} = [\sigma^2(F_o) + (0.015F_o)^2]$ was employed for both crystals. The final difference Fourier maps showed no residual peaks >0.8 e Å^{-3} for **1** and >0.4 e Å^{-3} for **2** with most of the largest peaks occurring about Cu and Cl atoms. Atomic scattering factors and anomalous dispersion terms were taken from ref 17. All calculations were carried out on a HITACHI M-680H computer at the Computer Center of the Institute for Molecular Science by using the program system UNICS III.[18]

The bond lengths and angles for **1** and **2** are given in Tables II and III, respectively.

Results

Solution Equilibria. The calculated stability constants log β_{pqrs} of the binary and ternary systems are shown in Tables IV and V, respectively.

The tendency of ternary complex formation can be evaluated by the use of Δ log *K* values as defined by[19]

(15) Gans, P.; Sabatini, A.; Vacca, A. *J. Chem. Soc., Dalton Trans.* **1985**, 1195–1200.

(16) These values are within the ranges reported previously (Sigel, H.; Zuberbühler, A. D.; Yamauchi, O. *Anal. Chim. Acta* **1991**, *255*, 63–72).

(17) Ibers, J. A., Hamilton, W. C., Eds. *International Tables for X-Ray Crystallography*; Kynoch: Birmingham, U.K., 1974; Vol. IV.

(18) Sakurai, T.; Kobayashi, K. *Rikagaku Kenkyusho Houkoku* **1979**, *55*, 69–77.

(19) Sigel, H. *Angew. Chem., Int. Ed. Engl.* **1975**, *14*, 394–402.

Table IV. Stability Constants (log β_{pqrs}) of Binary Complexes of A and B at 25 °C and I = 0.1 M (KNO_3)[a]

	log β_{pqrs}	
pqrs	EDMA	DL-DAP
1101	16.25(3)	15.683(3)
1100	13.473(6)	11.136(18)
1,1,0,−1	4.298(7)	
1,1,0,−2	−7.56(5)	
1202		29.952(28)
1201	26.5(1)	25.375(7)
1200	21.16(1)	20.057(2)
0101	9.870(3)	9.432(2)
0102	16.772(4)	16.166(2)
0103	18.93(1)	16.97(7)

	log β_{pqrs}			
pqrs	L-Ala	L-Arg	L-Lys	L-Val[b]
1010	8.211(1)	7.652(1)		8.049
1011			18.349(1)	
1,0,2,−1		3.14(1)		
1020	15.072(1)	14.128(1)	15.205(3)	14.913
1021			25.647(3)	
1022			35.547(1)	
0011	9.737(2)	9.104(1)	10.638(4)	9.573
0012	12.032(5)	11.099(1)	19.843(4)	
0013			21.84(2)	

[a] Values in parentheses denote standard deviations. [b] Data taken from: Brookes, G.; Pettit, L. D. *J. Chem. Soc., Dalton Trans.* **1977**, 1918–1924.

$$\mathrm{Cu(A)} + \mathrm{Cu(B)} \overset{10^{\Delta \log K}}{\rightleftharpoons} \mathrm{Cu(A)(B)} + \mathrm{Cu}$$

$$\Delta \log K = \log \beta_{\mathrm{Cu(A)(B)}} - \log \beta_{\mathrm{Cu(A)}} - \log \beta_{\mathrm{Cu(B)}} \quad (2)$$

where log $\beta_{Cu(A)(B)}$ etc. refer to the overall stability constants of the complexes indicated.

The statistical value for the systems containing Cu(II) and bidentate ligands is considered to be −0.9[19] due to the Jahn–Teller distortion, and lower values may indicate an unfavorable combination of ligands or the presence of a tridentate ligand. The $\Delta \log K$ values for the systems Cu(EDMA)(B) and Cu(DAP)(B) were calculated from the log β_{pqrs} values to be −2.16 to −2.47 and −0.89 to −1.72, respectively, which are much lower than those for Cu(en)(B) (−0.75 to −0.90). For both Cu(EDMA)(B) and Cu(DAP)(B), the $\Delta \log K$ values for B = L-Arg and L-Lys are significantly higher than those for B = L-Ala and L-Val, suggesting the contribution of a favorable intramolecular ligand–ligand interaction.

Evaluation of the stability enhancement of ternary complexes can be made by considering the following hypothetical equilibrium of complexes involving ligands with and without an interacting side chain group:[9g,h]

$$\mathrm{Cu(A)(L\text{-}Ala)} + \mathrm{Cu(en)(B)} \overset{K}{\rightleftharpoons} \mathrm{Cu(A)(B)} + \mathrm{Cu(en)(L\text{-}Ala)}$$

$$\log K = \log \beta_{\mathrm{Cu(A)(B)}} + \log \beta_{\mathrm{Cu(en)(L\text{-}AlA)}} - \log \beta_{\mathrm{Cu(A)(L\text{-}Ala)}} - \log \beta_{\mathrm{Cu(en)(B)}}$$

$$= \Delta \log K_{\mathrm{Cu(A)(B)}} + \Delta \log K_{\mathrm{Cu(en)(L\text{-}Ala)}} - \Delta \log K_{\mathrm{Cu(A)(L\text{-}Ala)}} - \Delta \log K_{\mathrm{Cu(en)(B)}} \quad (3)$$

where A refers to EDMA or DAP and B to L-Arg or L-Lys and ligand–ligand interactions are possible only in Cu(A)(B). The log K value (eq 3) is defined to be equal to zero when there is no ligand–ligand interaction.[9k] It is then possible to calculate log K values by using the stability constants listed in Table V with log K for Cu(en)(L-Ala) as the standard. By this formulation, we can maintain the factors such as the ligand field and steric requirements nearly the same on both sides of the equilibrium and thus evaluate the stabilization mainly due to ligand–ligand interactions.

Table V. Stability Constants (log β_{pqrs}) and $\Delta \log K$ and log K Values of Ternary Complexes, $Cu_p(A)_q(B)_rH_s$, at 25 °C and I = 0.1 M (KNO_3)[a]

ligand		species			
A	B	*pqrs*	log β_{pqrs}	$\Delta \log K$	log K
EDMA	L-Ala	1110	19.214(3)	−2.47	0.00
	L-Arg	1110	18.961(7)	−2.16	0.15
	L-Lys	1111	29.500(3)	−2.32	0.14
	L-Val	1110	19.152(3)	−2.37	0.05
DL-DAP	L-Ala	1110	17.906(9)	−1.44	0.00
	L-Arg	1110	18.135(6)	−0.65	0.63
	L-Lys	1111	28.204(8)	−1.28	0.16
	L-Val	1110	17.710(7)	−1.48	−0.09
en	L-Ala	1110		−0.90[b]	
	L-Arg	1110		−0.75[b]	
	L-Lys	1111		−0.90[b]	
	L-Val	1110		−0.85[b]	

[a] Values in parentheses denote standard deviations. [b] Data taken from: Odani, A.; Yamauchi, O. *Inorg. Chim. Acta* **1984**, *93*, 13–18.

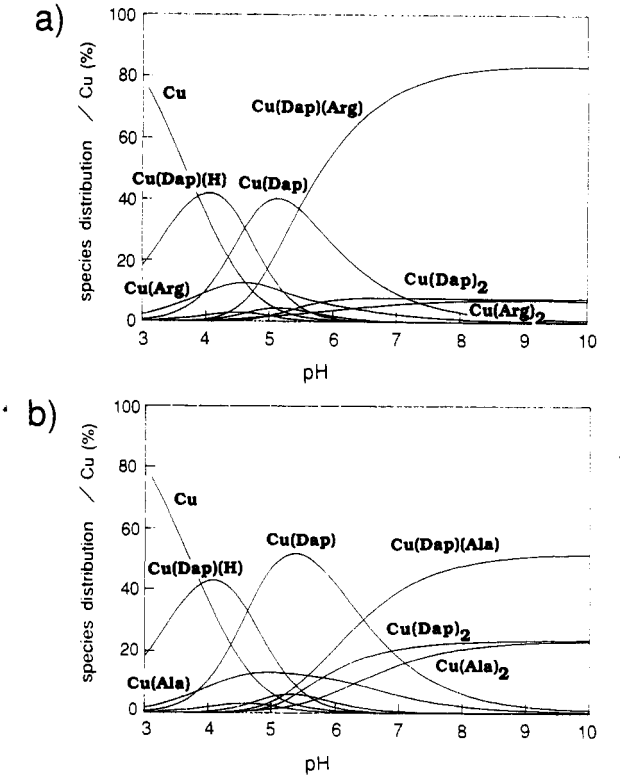

Figure 1. Species distributions as a funciton of pH calculated for 2 mM Cu(DAP)(L-Arg) (a) and 2 mM Cu(DAP)(L-Ala) (b) by using the stability constants listed in Tables VI and VII. The numbers of the curves denote species $Cu_p(A)_q(B)_rH_s$ expressed as *pqrs*.

We see from Table V that the log K values are positive for the complexes with B = L-Arg or L-Lys, whereas they are close to zero when B is L-Val, which is devoid of interacting groups. The results indicate that the complexes Cu(A)(L-Arg or L-Lys) are stabilized relative to Cu(A)(L-Ala) by ligand–ligand interactions, the order being Cu(DAP)(L-Arg) > Cu(EDMA)(L-Arg) ~ Cu(EDMA)(L-Lys) ~ Cu(DAP)(L-Lys) > Cu(EDMA)(L-Val) ~ Cu(DAP)(L-Val) ~ 0.

Absorption and CD Spectra. Absorption spectral data for the binary and ternary systems, $Cu(B)_2$ and Cu(A)(B), respectively, are shown in Table VI. Both systems in aqueous solution exhibit a d–d absorption peak at 585–622 nm at pH 8. The corresponding CD spectra have a negative extremum at 574–620 nm due to the vicinal effect of the asymmetric carbon of the optically active amino acids. The species distribution curves such as shown in Figure 1 confirm that these spectra correspond mainly to the ternary complexes, although there are contributions from the

Table VI. CD Spectral Data for Cu(A)(B) Systems in Water (I = var) and 50% (v/v) Aqueous Ethanol at pH 8 and Their Concentration Dependences

			H_2O		50% EtOH–H_2O	
system[a]	c/mM	λ_{max}/m	$\Delta\epsilon$	rel magnitude[b]	$\Delta\epsilon$	rel magnitude[b]
Cu(EDMA)(L-Arg)	2	606	–0.098	1.8	–0.16	3.0
	10		–0.100	1.7	–0.16	2.8
	100		–0.098	1.9	–0.14	2.9
Cu(EDMA)(L-Lys)	2	607	–0.092	1.5	–0.13	2.3
	10		–0.097	1.4	–0.13	2.2
	100		–0.093	1.2	–0.11	1.4
Cu(EDMA)(L-Ala)	2	610	–0.052	1.2	–0.07	1.3
	10		–0.048	1.1	–0.07	1.3
	100		–0.050	1.1	–0.06	
Cu(DAP)(L-Arg)	2	580	–0.076	1.4	–0.10	1.9
	10		–0.075	1.2	–0.09]	1.6
	100		–0.072	1.4	–0.08	1.7
Cu(DAP)(L-Lys)	2	595	–0.078	1.2	–0.09	1.6
	10		–0.075	1.1	–0.08	1.4
	100		–0.076	1.0	–0.08	1.1
Cu(DAP)(L-Ala)	2	620	–0.043	0.9	–0.05	1.0
	10		–0.040	0.9	–0.05	1.0
	100		–0.042	0.9	–0.04	

[a] The CD spectral data for Cu(L-B)$_2$ in water are as follows: L-Arg, –0.14; L-Lys, –0.13; L-Ala, –0.11. [b] Relative CD magnitude is defined as $\Delta\epsilon_{obsd}/\Delta\epsilon_{calcd}$. $\Delta\epsilon_{calcd}$ is equal to $\Delta\epsilon_{Cu(L\text{-}B)_2}/2$.

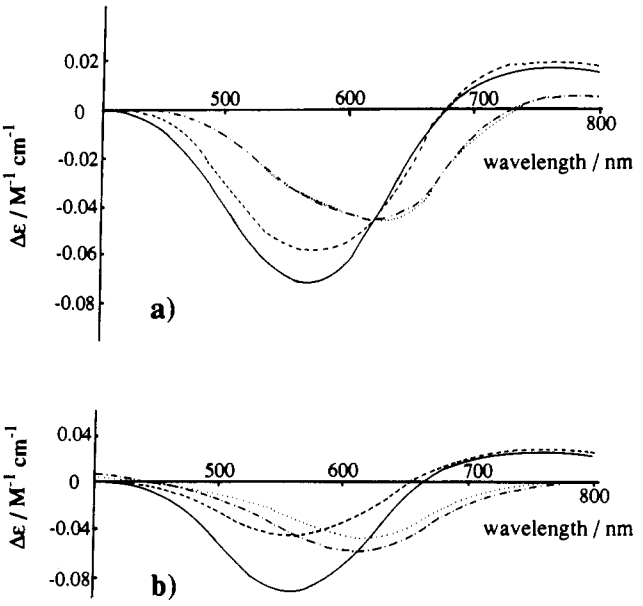

Figure 2. Observed and calculated CD spectra for the Cu(DAP)(L-Arg) and Cu(DAP)(L-Ala) systems in water (a) and 50% ethanol–water (b). Cu(DAP)(L-Arg): observed (—); calculated (- - -). Cu(DAP)(L-Ala): observed (- · -); calculated (···). The spectra in the visible region were calculated according to eq 4. Concentration: 2 mM.

binary species. The spectral data for Cu(EDMA)(B) are in good agreement with those reported previously.[9a]

In the absence of ligand–ligand interactions, the CD spectral magnitudes for ternary Cu(II)–amino acid complexes Cu(A)(B) are an additive function of the magnitudes for the binary complexes of the amino acids, Cu(A)$_2$ and Cu(B)$_2$. Martin[20] observed the magnitude additivity for Cu(II)–dipeptide complexes, where the magnitude can be estimated from the magnitudes for the complexes of the component amino acids. Thus, we may expect the magnitude $\Delta\epsilon_{calcd}$ for Cu(L-A)(L-B) according to eq 4,[9a] where

$$\Delta\epsilon_{calcd} = {}^1/_2(\Delta\epsilon_{Cu(L\text{-}A)_2} + \Delta\epsilon_{Cu(L\text{-}B)_2}) \qquad (4)$$

$\Delta\epsilon_{Cu(L\text{-}A)_2}$ and $\Delta\epsilon_{Cu(L\text{-}B)_2}$ are the magnitudes for the binary complexes at the maximum wavelength of Cu(L-A)(L-B). For complexes with optically inactive A, such as EDMA and DL-DAP, the $\Delta\epsilon_{calcd}$ is simply equal to ${}^1/_2\Delta\epsilon_{Cu(L\text{-}B)_2}$. Ligand–ligand interactions between the side chains of A and B give rise to magnitude anomaly, the ratio of the observed magnitude $\Delta\epsilon_{obsd}$ to $\Delta\epsilon_{calcd}$ (relative magnitude = $\Delta\epsilon_{obsd}/\Delta\epsilon_{calcd}$) deviating from 1 (Figure 2a).

The CD spectral data in the d–d region and relative magnitudes summarized in Table VI show that the magnitudes at 580–620 nm for Cu(A)(L-Arg) are nearly independent of the concentrations, whereas those for the systems with B = L-Lys decrease at higher concentrations. The relative magnitudes are larger for Cu(A)(B) (B = L-Arg, L-Lys) than for Cu(A)(L-Ala), which are close to 1.0 (0.9–1.2). They are further enhanced in 50% aqueous ethanol as typically illustrated by the spectrum for Cu(DAP)(L-Arg) in Figure 2b. On the basis of our previous experimental evidence,[9] these magnitude enhancements are concluded to be due to the electrostatic ligand–ligand interactions in Cu(A)(B).

Molecular Structure of [Cu(EDMA)(L-Arg)ClO$_4$]·1/2C$_2$H$_5$OH (1). Figure 3 shows a perspective view of **1**, with the atomic labeling scheme in the asymmetric unit. The coordination environment around the copper atom is considered to be a slightly distorted square pyramid with the two nitrogens of EDMA and the amino nitrogen and the carboxylate oxygen of L-Arg at the equatorial positions (Cu–N(1) = 2.018(13), Cu–N(2) = 1.988(16), Cu–N(3) = 1.995(15), Cu–O(1) = 1.932(13) Å) and the carboxylate oxygen of EDMA at an axial position (Cu–O(3) = 2.337(13) Å). The perchlorate ion weakly coordinates to the remaining axial position through one of the oxygen atoms (Cu–O(5) = 2.83(15) Å). The three nitrogens and the Arg carboxylate oxygen coordinated to Cu(II) are planar to within 0.15 Å. The dihedral angle between the plane defined by the copper atom and two nitrogen atoms of EDMA and that defined by the copper atom and the nitrogen and oxygen atoms of L-Arg is 15.4°, showing the twisting of the coordination plane which favors the axial coordination of the EDMA carboxylate oxygen. The copper atom deviates by 0.10 Å from the coordination plane toward this oxygen.

The most important structural feature of **1** is the existence of a specific interaction between the Arg guanidinium group of one complex molecule and the EDMA carboxylate group of a neighboring molecule through the two parallel N–H···O hydrogen bonds of type A according to the definition by Salunke and Vijayan.[21] These intermolecular interactions form an infinite chain of the complex molecules in the crystal structure, which is considered to be necessary for crystal growth. Somewhat similar

(20) Tsangaris, J. M.; Martin, R. B. *J. Am. Chem. Soc.* **1970**, *92*, 4255–4260. R. B. Martin. *Met. Ions Biol. Syst.* **1974**, *1*, 129–156.

(21) Salunke, D. M.; Vijayan, M. *Int. J. Pept. Protein Res.* **1981**, *18*, 348–351.

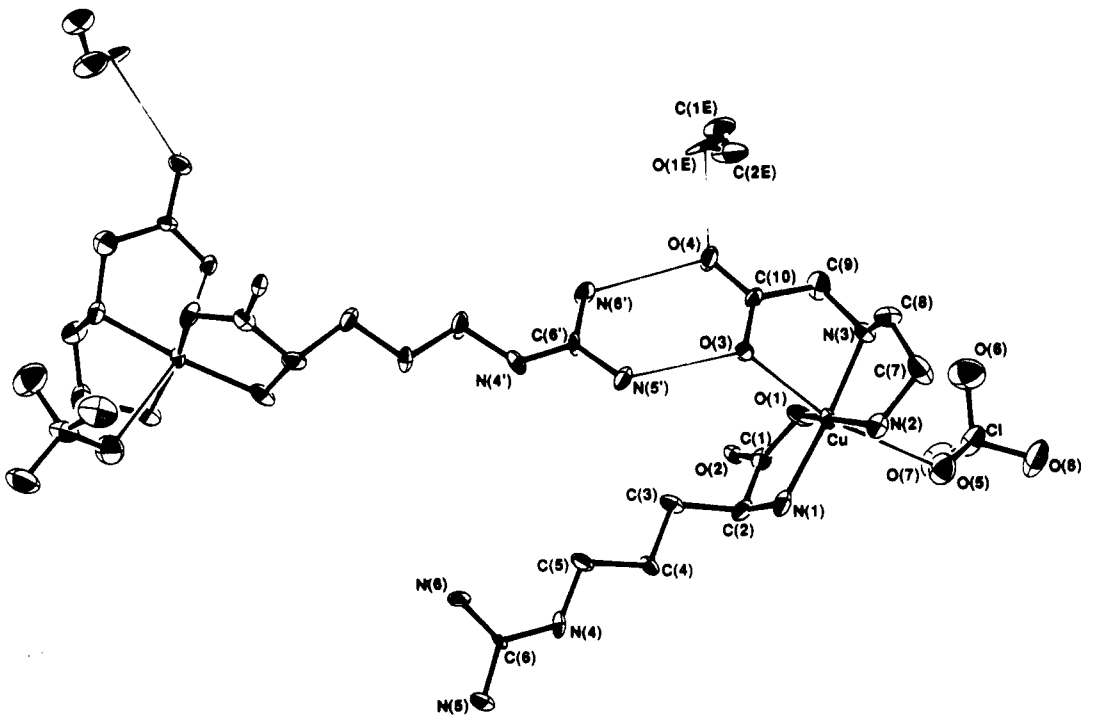

Figure 3. Molecular structure of [Cu(EDMA)(L-Arg)ClO_4] in **1** with the atomic labeling scheme in the asymmetric unit. The primed atoms are related to the unprimed atoms by the crystallographic screw axis.

intermolecular guanidinium–carboxylate bonds have been reported for [Cu(L-Arg)$_2$(acetate)$_2$],[22] where the carboxylate group of an axially coordinated acetate ion is hydrogen-bonded to the guanidinium group of a neighboring complex in the type B mode.[21] The hydrogen bonds in the present case are formed between the side chains of the coordinated ligands from neighboring complex molecules. The distances are 2.89 and 2.85 Å for O(3)···N(5′) and O(4)···N(6′), respectively, which are comparable with those of the L-arginine–acetate bonds in the above complex[22] and in the L-arginine–L-glutamate salt[23] (N···O = 2.90, 2.94[22] and 2.83, 2.85 Å[23]). The planes formed by the carboxylate group (C(10), O(3), O(4)) and by the guanidinium group (C(6), N(5), N(6)) are nearly coplanar to within 0.13 Å, and the torsion angle of N(5′)–N(6′)–O(3)–O(4) is 13.6°. The O(3)···O(4) (2.23 Å) and N(5)···N(6) (2.28 Å) separations are nearly equal, indicating that this combination may be the best fit for the functions of molecular recognition and specific binding by amino acid side chains.

Molecular Structure of [Cu(L-Arg)$_2$](NO$_3$)$_2$·3H$_2$O (2). The perspective view of **2** in the asymmetric unit along with the atomic labeling scheme is shown in Figure 4. The coordination around the copper is square-planar (Cu–O(1A) = 1.930(4), Cu–O(1B) = 1.973(5), Cu–N(2A) = 1.974(5), Cu–N(2B) = 1.972(5) Å), the plane defined by the two nitrogens and two oxygens from two L-Arg molecules being planar to within 0.02 Å. The copper atom is located only 0.06 Å above this plane and has no ligands at the axial positions. Interestingly the configuration around Cu(II) is cis with respect to the amino groups, which are hydrogen-bonded to a nitrate ion (Figures 4 and 5a). The L-Arg side chains are extended outward, and one of them is hydrogen-bonded to two nitrate ions through the guanidinium group in the type A and type B modes (Figure 5b).[21] The guanidinium–nitrate hydrogen bonds in this crystal have N···O distances of 2.84–2.97 Å (Figure 5b), which are comparable with those found in **1**, and the planes formed by the nitrate ion and the guanidinium group are nearly coplanar to within 0.13 Å. The O···O separations in the nitrate

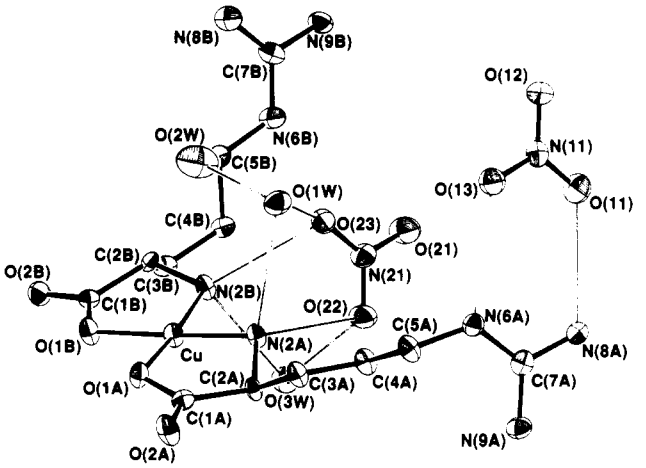

Figure 4. Molecular structure of **2** with the atomic labeling scheme in the asymmetric unit. The primed atoms are related to the unprimed atoms by the crystallographic screw axis.

ions (2.15–2.17 Å) and N···N separations in the guanidinium groups (2.29–2.31 Å) are also comparable with the respective values for **1**. The complex molecules are in an infinite three-dimensional network of hydrogen bonding through the guanidinium group, nitrate ion, and water molecules in the crystal structure.

Discussion

Modes of Electrostatic Ligand–Ligand Interactions. It has been concluded previously that Cu(EDMA)(L-B) (B = Arg or Lys) involves the side chain electrostatic interactions or hydrogen bonds that give rise to CD magnitude anomaly.[9a] The present spectral and structural findings substantiate the previous conclusion regarding such interactions and further support their existence also in the Cu(DAP)(B) systems. On the basis of the CD spectral anomaly and the previous ^{1}H NMR spectral studies, as well as the present X-ray studies, we may infer that the guanidinium–carboxylate interactions most probably take place *within* the complex molecule when Cu(EDMA)(L-Arg) and Cu(DAP)(L-Arg) are in solution.

(22) Duarte, M. T. L. S.; Carrondo, M. A. A. F. d. C. T.; Goncalves, M. L. S. S.; Hursthouse, M. B.; Walker, N. P. C.; Dawes, H. M. *Inorg. Chim. Acta* **1986**, *124*, 41–47.
(23) Bhat, T. N.; Vijayan, M. *Acta Crystallogr.* **1977**, *B33*, 1754–1759.

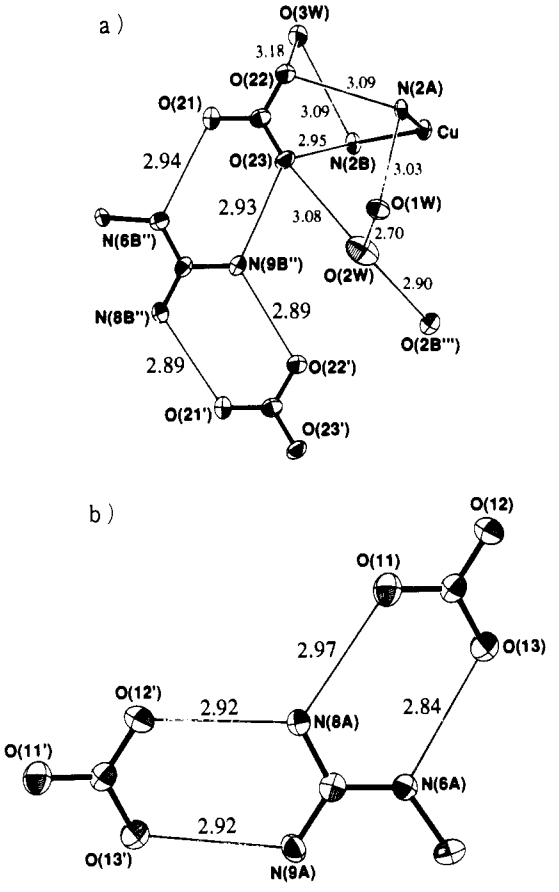

Figure 5. Hydrogen-bonding network involving the Arg guanidinium and amino groups, nitrate ions, and water molecules (a) and two types of guanidinium–nitrate bonding (b) in **2**.

The magnitude anomaly as judged from the relative magnitudes, $\Delta\epsilon_{obsd}/\Delta\epsilon_{calcd}$, is less prominent for Cu(DAP)(B) and more concentration dependent for Cu(A)(L-Lys). If we simply assume that the degree of deviation of the relative magnitude from 1.0 is proportional to the extent of the conformational change from the strain-free state of L-B in the binary complex, the values for Cu(DAP)(B) imply that the intramolecular ligand–ligand interactions take place without serious conformational changes; i.e., the steric requirements are more favorable for the interactions in Cu(DAP)(B) than for those in Cu(EDMA)(B). Figure 3 and space-filling molecular models indicate that, owing to the coordination of N(3) and probably O(3), the carboxylate group of EDMA cannot easily adjust the orientation of the oxygen atoms to the guanidinium group to form hydrogen bonds. The DAP carboxylate group, on the other hand, can assume the ideal conformation for the bonding because of the flexibility arising from the puckering of the chelate ring and free rotation around the C–C bond in the absence of restrictions due to axial coordination. As described in the previous section, the coordination plane of **1** is twisted to accommodate the axial coordination. Studies of molecular models suggest that the intramolecular guanidinium···carboxylate bonding gives rise to a strain in the Cu(EDMA)(L-Arg) coordination structure, whereas it is strain-free or well aligned in Cu(DAP)(L-Arg) (Figure 6).

On the other hand, the relative magnitudes for Cu(A)(L-Lys) are more concentration dependent than those for Cu(A)(L-Arg) (Table VI). This may be partly due to the shorter side chain length of Lys but may also indicate that the bonding of the Lys ammonium group is less sensitive to the bond directions and thus less specific and more electrostatic, so that at higher concentrations it may be involved in the interactions with the carboxylate groups of neighboring complex molecules. The mentioned differences due to A and B are reflected in the log K values (eq 3, Table V) as a measure of stabilization due to ligand–ligand interactions:

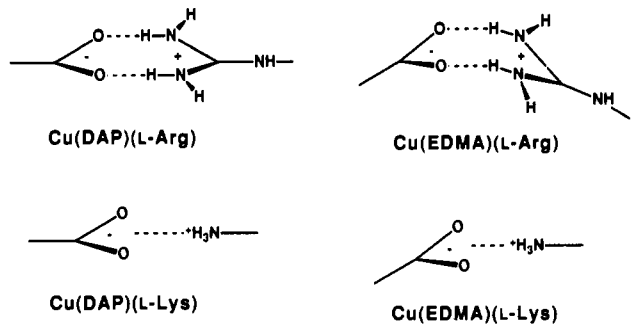

Figure 6. Steric requirements for electrostatic or hydrogen bondings between side chain groups in ternary complexes Cu(A)(B).

Comparison between the log K values for Cu(EDMA)(L-Arg) and Cu(DAP)(L-Arg) clearly shows that formation of the latter is much more favored over the former mainly for steric reasons. The smaller values for Cu(A)(L-Lys) may indicate that the interactions involving the Lys ammonium group are weaker or less effective. Twisting of the guanidinium–carboxylate alignment as shown in Figure 6 may increase the electrostatic nature of the bond and explain why the Lys-containing complexes Cu(A)(L-Lys) which are capable of both electrostatic and hydrogen bondings have a similar stability irrespective of A. Thus, the interactions involving Lys are inferred to be less affected by the steric requirements for the interactions.

The guanidinium–nitrate bonds in **2** (Figure 5) point out the possiblity that the nitrate ion is an efficient hydrogen-bonding partner not only of the guanidinium group but also of the amino groups coordinated in the cis positions, as shown in Figures 4 and 5a, or similar vicinal groups. This ion may have contributed to the cis configuration of complex **2**.

Concluding Remarks and Biological Implication. Although weak interactions are affected by the medium, i.e. the ionic strength, pH, and concentration, they are still present in aqueous solutions of millimolar concentrations, as seen from the above mentioned spectral and thermodynamic findings. The guanidinium–carboxylate bonding of the type found in **1** has been revealed between the Arg and aspartyl residues near the active site of *Pseudomonas putida* cytochrome P-450.[24] Because the guanidinium and ammonium groups can offer all the hydrogen atoms that are necessary for hydrogen bonding, their biological partners may be carboxyl and carbonyl oxygens, phosphate oxygens, water and hydroxyl oxygens, aromatic nitrogens, etc.

In this regard, the importance of Arg residues has previously been discussed in connection with biological functions such as in the CPA–peptide bonding,[3] the guanidinium–phosphate interactions at the active site of Staphylococcal nuclease,[25] and superoxide binding in Cu,Zn-superoxide dismutase.[26-28] A central role played by the Arg guanidinium–phosphate interactions was disclosed by X-ray analysis of the phosphorylase–heptulose 2-phosphate complex.[29] RNA recognition through the "arginine fork" defined as the interaction between a guanidinium group and adjacent pairs of phosphates of RNA has been proposed recently.[30] Guanidinium–carboxylate interactions in protected

(24) Poulos, T. L.; Finzel, B. C.; Howard, A. J. *Biochemistry* **1986**, *25*, 5314–5322.
(25) Cotton, F. A.; Day, V. W.; Hazen, E. E., Jr.; Larsen, S.; Wong, S. T. K. *J. Am. Chem. Soc.* **1974**, *96*, 4471–4478.
(26) (a) Cudd, A.; Fridovich, I. *J. Biol. Chem.* **1982**, *257*, 11443–11447. (b) Getzoff, E. D.; Tainer, J. A.; Weiner, P. K.; Kollmann, P. A.; Richardson, J. S.; Richardson, D. C. *Nature* **1983**, *306*, 287–290.
(27) (a) Mota de Freitas, D.; Luchinat, C.; Banci, L.; Bertini, I.; Valentine, J. S. *Inorg. Chem.* **1987**, *26*, 2788–2791. (b) Mota de Freitas, D.; Valentine, J. S. *Biochemistry* **1984**, *23*, 2079–2082.
(28) Banci, L.; Bertini, I.; Luchinat, C.; Hallewell, R. A. *J. Am. Chem. Soc.* **1988**, *110*, 3629–3633.
(29) Johnson, L. N.; Acharya, K. R.; Jordan, M. D.; McLaughlin, P. J. *J. Mol. Biol.* **1990**, *211*, 645–661.
(30) Calnan, B. J.; Tidor, B.; Biancalana, S.; Hudson, D.; Frankel, A. D. *Science* **1991**, *252*, 1167–1171.

arginylglutamate and the guanidinium–guanine hydrogen bonds in the presence of guanine were previously concluded from NMR studies.[31]

Studies on simple chemical systems offer valuable information on the mode and energy of weak interactions between molecules. Since metal ions place the interacting molecules close to each other and transmit information on the metal–ligand bonding through their electronic spectra etc., mixed-ligand–metal complexes with ligand–ligand interactions may be regarded as the prototype of weak interactions of biological interest.

(31) Lancelot, G.; Mayer, R.; Hélène, C. *J. Am. Chem. Soc.* **1979**, *101*, 1569–1576.

Acknowledgment. We thank Tamotsu Sugimori and Kana Kaneshiro for assistance with the experiments. This work was supported by a Grant-in-Aid for Scientific Research (No. 02453039) and a Grant-in-Aid for Scientific Research on Priority Areas (No. 03241101) from the Ministry of Education, Science, and Culture of Japan, for which we express our thanks.

Supplementary Material Available: Tables of atomic coordinates and isotropic thermal parameters for non-hydrogen atoms, anisotropic temperature factors for non-hydrogen atoms, positional parameters for hydrogen atoms, and torsion angles (5 pages). Ordering information is given on any current masthead page. Observed and calculated structure factors are available from the authors upon request.